Calibration of Reactive Transport Models for Remediation of Mine Drainage in Solid-Substrate Biocolumns

Paulo S. Hemsi, Ph.D.[1]; Charles D. Shackelford, Ph.D., M.ASCE[2]; and Linda A. Figueroa, Ph.D., M.ASCE[3]

Abstract: Experimental data pertaining to two pairs of solid-substrate sulfate-reducing biocolumns for remediation of mine drainage were used for calibrating and testing new reactive transport models based on sulfate reduction and sulfide precipitation linked to rate-limiting solid-substrate hydrolysis. First-order (F) and Contois (C) kinetics for decomposition as well as different numbers of pools of decomposable materials were proposed in different models (F1–F3 and C1–C3). Effluent sulfate concentrations for one of the columns were used as the basis for calibrating the different models and, due to limitations in the calibration data set, the number of adjustable model parameters was limited using parameter tying. Calibrated models were ranked using Akaike information criterion, and Model C2, followed by Model C1, based on Contois kinetics, emerged as the models that were supported to a greater extent by the data. For an independent experimental data set, model testing was performed using Models C2 and C1 with parameters from the previous calibration resulting in good approximations of effluent sulfate. For the calibration data set, longer-term model predictions for effluent sulfate, decomposable substrates, and microbial populations also were performed. The reactive transport models represent a potentially valuable tool for the design of solid-substrate bioreactors used for the treatment of mining influenced water, although future model validation using longer-term field data sets will be necessary to confirm the model predictions.

DOI: 10.1061/(ASCE)EE.1943-7870.0000234

CE Database subject headings: Calibration; Mining; Models; Organic matter; Sulfate; Wastewater management.

Author keywords: Mining influenced water; Modeling; Solid organic substrates; Sulfate reduction.

Introduction

Abandoned mine land (AML) sites are frequently remote and characterized by problems associated with mining influenced water, such as acid mine drainage (AMD), i.e., low pH water laden with metals from mine tunnels, mill tailings, and waste rock. Such AMD represents a significant environmental problem in terms of impacting streams and groundwater aquifers. For example, approximately 51,700 AML sites are located within only six states of U.S. EPA Region 8 (WGA 1998). Remediation of such mining influenced water can be accomplished via the use of passive treatment systems such as passive bioreactors and permeable reactive barriers. Such elements can be installed to intercept and passively treat contaminated groundwater down gradient from a contaminant source (Benner et al. 1999; Groudev et al. 2003; Whitehead et al. 2005).

In particular, the use of decomposable organic solids to provide slow release of organic substrates in support of biogenic sulfide production and metal-sulfide precipitation in engineered biogeochemical systems allows for low-cost, low-maintenance remediation of mining influenced water at AML sites. For example, the results of several laboratory studies involving sulfate-reducing (SR) flow-through experiments for metal precipitation have demonstrated the potential use of sulfate reduction and metal-sulfide precipitation coupled to the decomposition of organic solids for the remediation of mining influenced water (e.g., Gibert et al. 2004). Examples of solid, decomposable organic materials that have been evaluated for this purpose include sawdust (Tuttle et al. 1969; Wakao et al. 1979), spent mushroom compost (Dvorak et al. 1992; Hammack and Edenborn 1992), fresh alfalfa (Bechard et al. 1994), leaf mulch and wood chips (Waybrant et al. 1998; Chang et al. 2000), and corn stover (Figueroa et al. 2007). Also, some field applications of SR systems in permeable reactive barriers, wetlands, and large-scale bioreactors have been reported (Benner et al. 1999; Groudev et al. 2003; Whitehead et al. 2005).

The design of SR field applications historically has been based on short-term laboratory experiments focusing primarily on changes in inorganic chemistry. Advances in design and predictability are expected to result from enhancing the characterization of suitable organic material, monitoring changes in organic chemistry (e.g., organic substrates) and biological components (e.g., microbial ecology) (Hallberg and Johnson 2005; Place et al. 2006; Pruden et al. 2006), and developing and calibrating biogeochemical simulation tools that include major aspects of the system. Conceptual models for the microbial ecology in SR systems range from complex with multiple linked microbial processes to simpler single process models.

The flowchart shown in Fig. 1, which was used as the basis for the mathematical models presented in this study, includes the hydrolysis of polysaccharides, sulfate reduction based on lactate, and precipitation of metal sulfides. The multiple possible path-

[1]Professor, Div. of Civil Engineering, Aeronautics Institute of Technology, São José dos Campos, SP 12.228-900, Brazil (corresponding author). E-mail: paulosh@ita.br

[2]Professor, Dept. of Civil and Environmental Engineering, Colorado State Univ., 1372 Campus Delivery, Fort Collins, CO 80523-1372.

[3]Associate Professor, Div. of Environmental Science and Engineering, Colorado School of Mines, Coolbaugh Hall, Golden, CO 80401-1887.

Note. This manuscript was submitted on March 24, 2009; approved on February 3, 2010; published online on February 8, 2010. Discussion period open until February 1, 2011; separate discussions must be submitted for individual papers. This paper is part of the ***Journal of Environmental Engineering***, Vol. 136, No. 9, September 1, 2010. ©ASCE, ISSN 0733-9372/2010/9-914–925/$25.00.

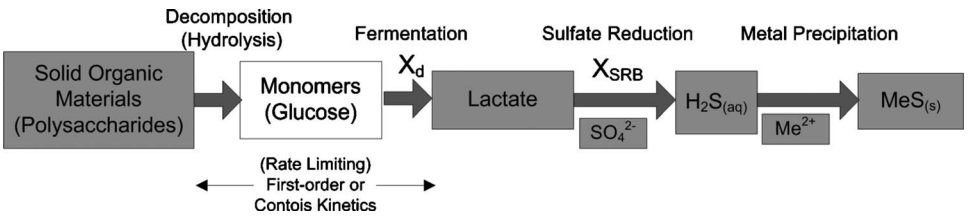

Fig. 1. Flowchart of sequential biochemical processes in the mathematical models for models based on first-order and Contois kinetics for hydrolysis

ways for the degradation of complex organic matter were simplified to a model biopolymer (polysaccharide) and a model intermediate compound (lactate), which is analogous to the approach used for the development of activated sludge models (Henze et al. 2000).

More broadly, decomposer groups catalyze the hydrolysis of complex organic materials (e.g., cellulose, protein, lipids) and the fermentation of the hydrolysis products (e.g., glucose) to simpler compounds (e.g., acetate or lactate) (Colberg 1988). The simpler compounds serve as the carbon and energy source for SR bacteria. Fermentation and sulfate reduction require reduced conditions as indicated by the negative redox potential ($pe < -3$) required for both reactions (Zehnder and Stumm 1988). The pH preference of sulfate reducers has been reported as $6 \leq \text{pH} \leq 9$ (Widdel 1988). The pH optimum for the anaerobic digestion of solid organic materials is in a similar range of $6.5 \leq \text{pH} \leq 8.2$ (Speece 1996). The maximum reported rates of sulfate reduction and fermentation are at temperatures above 30°C. Thus, at environmentally relevant temperatures ($\geq 2°\text{C}$), measurable but slower rates of sulfate reduction are observed (Widdel 1988).

In terms of modeling the rate of sulfate (SO_4^{2-}) reduction, Monod kinetics (Monod 1949) has been used to take into account the growth of SR bacteria in some models (Schafer et al. 1998; Prommer et al. 2001; Mayer et al. 2002). However, these models only considered scenarios where soluble organic substrates (e.g., ethanol, lactate) were injected directly or amended to the media. Sustainable systems will be based on the decomposition of solid organic materials as a prerequisite to releasing dissolved bacterial substrates and rate limiting to bioremediation (Tuttle et al. 1969). Although other models have accounted for the linkage between SO_4^{2-} reduction and the rate of organic material decomposition (e.g., Westrich and Berner 1984; Drury 2000), these models have been based only on first-order kinetics and have neglected bacterial fate and surface-limiting considerations.

Recent data from SR biocolumns based primarily on corn stover presented herein are used for calibrating and testing the modeling approaches described subsequently, which are based on modeling sulfate reduction and metal precipitation coupled to solid-phase decomposition (hydrolysis). This study represents an extension of a previous study that evaluated the use of the models to simulate the results of batch equilibrium (no-flow) SR systems (Hemsi et al. 2005). The issue of long-term biocolumn longevity also is addressed with the models, which include the fates of solid decomposable materials and the decomposer bacterial population.

Development of Models

As illustrated in Fig. 1, the chemical and biological processes in the models proposed in this study include the following: (1) anaerobic hydrolysis (decomposition) of polysaccharides in solid organic materials due to the activity of a consortium of generally designated decomposer bacteria (X_d); (2) SO_4^{2-} reduction based on incomplete oxidation of lactate; and (3) precipitation of metal sulfides due to the release of H_2S (hydrogen sulfide). In the models, the rate of sulfate reduction and, consequently, that of metal precipitation is linked to the rate-limiting step of polysaccharide (cellulose and hemicellulose) decomposition (Tuttle et al. 1969; Westrich and Berner 1984; Bechard et al. 1994; Chynoweth and Pullammanappallil 1996; Drury 2000). In turn, polysaccharide decomposition and release of soluble substrates are limited by the extent of solid-phase hydrolysis (Vasiliev et al. 1993; Vavilin et al. 2004; Batstone et al. 2002), which becomes the most significant component in mathematical models representing such biochemical systems.

Solid-Phase Hydrolysis

In contrast with the more complex, mechanistic solid-hydrolysis kinetics (e.g., Humphrey 1979), relatively simple first-order and Contois kinetics (Contois 1959) are commonly applied to simulate the anaerobic digestion of organic matter (e.g., Vasiliev et al. 1993; Rittmann and McCarty 2001; Vavilin et al. 2004). Based on first-order kinetics, the rate of hydrolysis, which is the slowest step in polysaccharide decomposition, can be expressed as follows:

$$\frac{d[CE_i]}{dt} = -k_{f,i}[CE_i] \tag{1}$$

where $[CE_i]$=remaining concentration of decomposable polysaccharide i in terms of dry mass per volume of solution (g/L), $k_{f,i}$ =hydrolysis rate coefficient (d^{-1}), and t=time.

In a surface-limiting process, such as Contois kinetics, the time rate of solid-substrate hydrolysis may decrease as the biomass concentration of decomposer bacteria increases above a limiting level, reflecting surface area and mass transfer limitations. Based on Contois kinetics, the rate of hydrolysis is regulated by the ratio between the concentrations of the remaining decomposable polysaccharide and decomposer bacteria, as follows:

$$\frac{d[CE_i]}{dt} = -k_{c,i}[X_{d,i}]\frac{([CE_i]/[X_{d,i}])}{K_{A,i} + ([CE_i]/[X_{d,i}])} \tag{2}$$

$$\frac{d[X_{d,i}]}{dt} = -Y_{Xd/CE}\left(\frac{d[CE_i]}{dt}\right) - d_i[X_{d,i}] \tag{3}$$

where $[X_{d,i}]$=biomass concentration of the decomposer bacteria associated with material i (cell g total mass/L), $k_{c,i}$=Contois specific rate coefficient (d^{-1}), $K_{A,i}$=Contois affinity coefficient (g/g), $Y_{Xd/CE}$=stoichiometric mass-yield coefficient [see Eq. (4), $Y_{Xd/CE}$=0.183 g/g], and d_i=first-order decay coefficient for decomposer bacteria. In Eq. (2), the rate of polysaccharide decom-

position transitions between the two limiting cases of first-order kinetics with respect to $[CE_i]$ at low $[CE_i]/[X_{d,i}]$ ratios, and first-order kinetics with respect to $[X_{d,i}]$ at high $[CE_i]/[X_{d,i}]$ ratios (i.e., exponential $X_{d,i}$ growth). Rate coefficients such as k_f and k_c lump the effects of intrinsic material degradability properties, particle characteristics (gradation, surface area), and testing conditions, which are more explicit in more mechanistic models (Humphrey 1979).

Subsequent Steps

Dissolved Organic Substrate

The rate of release of a soluble organic substrate, such as lactate utilized by SR bacteria, can be taken to be directly proportional to the rate of solid decomposition, as well as the growth rate of decomposer bacterial biomass (X_d) [Eq. (3)]. The yield coefficients for proportionality were obtained from the following reaction derived using the half-reaction approach (Rittmann and McCarty 2001):

$$2\underbrace{C_6H_{10}O_5}_{\text{cellulose}} + 0.427H_2O + 0.524NH_4^+ \rightarrow 3.126\underbrace{C_3H_5O_3^-}_{\text{lactate}} + 3.652H^+ + 0.524\underbrace{C_5H_7O_2N}_{\text{biomass}} \quad (4)$$

where $C_5H_7O_2N$ represents an empirical formula for cells (Rittmann and McCarty 2001), and the stoichiometric mass-yield coefficients for lactate and biomass are $Y_{LA/CE}=0.859$ g/g and $Y_{Xd/CE}=0.183$ g/g, respectively.

Sulfate Reduction and Metal Precipitation

The rate of sulfate reduction is assumed to be directly proportional to the rate of release of lactate in solution, i.e., as long as SO_4^{2-} is present. Since the rate-limiting step is solid-substrate hydrolysis, sulfate reduction is assumed in the models to be sufficiently fast.

Stoichiometric mass-yield coefficients for $Y_{SO/LA}$ and $Y_{HS/LA}$ of 0.507 g/g and 0.180 g/g, respectively, were obtained based on the reaction for sulfate reduction on lactate obtained using the half-reaction approach (Rittmann and McCarty 2001):

$$2.128\underbrace{C_3H_5O_3^-}_{\text{lactate}} + SO_4^{2-} + 0.077NH_4^+ + 0.051H^+ \rightarrow 2HCO_3^- + 0.234H_2O + H_2S + \underbrace{2C_2H_3O_2^-}_{\text{acetate}} + 0.077\underbrace{C_5H_7O_2N}_{\text{biomass}} \quad (5)$$

An instantaneous-reaction approach is used, with the inherent assumption that any time an amount of the organic substrate (lactate) is produced at a given location within the biocolumn, this amount is transported and consumed in sulfate reduction, i.e., as long as the SO_4^{2-} concentration at the location is greater than $Y_{SO/LA}[LA]$, where $[LA]$ denotes the lactate concentration. In this case, the stoichiometric amounts of SO_4^{2-} and H_2S will be consumed and produced, respectively, at the cell in the model domain, in accordance with the following expressions:

$$[SO]=[SO]-Y_{SO/LA}[LA], \quad [HS]=[HS]+Y_{HS/LA}[LA] \quad (6)$$

where $[SO]$ and $[HS]$ represent sulfate and hydrogen sulfide concentrations, respectively, and the Y symbols represent the corresponding mass-yield coefficients. Since sulfate is present in the influent solution and, as previously described, is consumed only to the extent of lactate availability (i.e., the limiting reactant), SO_4^{2-} generally remains in excess along the column.

Similarly, the rate of metal-sulfide precipitation in the biocolumn is assumed to be directly proportional to the rate of release of H_2S, i.e., to be sufficiently fast, as long as metals are present. Any time an amount of H_2S is released at a given location within the biocolumn, this amount is transported and consumed in metal-sulfide precipitation, i.e., as long as metal concentrations at the location are greater than $Y_{ME/HS}[HS]$, where $[HS]$ denotes the hydrogen sulfide concentration and $Y_{ME/HS}$=a mass-yield coefficient for metal sulfide precipitation (e.g., ZnS, $Y_{ZN/HS}$ =1.919 g/g). The stoichiometric amount of metal will be removed in accordance with the following relation:

$$[ME]=[ME]-Y_{ME/HS}[HS] \quad (7)$$

Model Solution

The experiments are modeled as bioreactors, where the temporal rate of mass accumulation/removal for any species is equal to a combination of the mass production/consumption (reactions) within the reactor and the mass input/output (transport). For each species in the reactor, mass balance can be written generically as an advection-dispersion-reaction equation as follows:

$$\frac{\partial[c]}{\partial t}=\left(D_{xx}\frac{\partial^2[c]}{\partial x^2}+D_{yy}\frac{\partial^2[c]}{\partial y^2}+D_{zz}\frac{\partial^2[c]}{\partial z^2}\right)-\frac{\partial}{\partial x}(v[c]) + \left.\frac{\partial[c]}{\partial t}\right|_{\text{reactions}} \quad (8)$$

where t=time, x, y, and z=Cartesian coordinate axes, with x being parallel to the longitudinal direction of flow, $[c]$ =concentration of a generic species, D_{xx}, D_{yy}, and D_{zz}=principal components of the hydrodynamic dispersion tensor in the respective x, y, and z directions, v ($=q/n$, where q=liquid flux or Darcy velocity, and n=total porosity) is the seepage velocity parallel to the x direction, and $\partial[c]/\partial t|_{\text{reactions}}$=temporal net rate of mass utilization given by biochemical processes as previously discussed. As explained later, the value of n was assumed to be 0.73. The values of v used for simulation were adjusted based on the experimental value by adjusting the values of hydraulic conductivity K and hydraulic gradient i (i.e., $q=Ki$). Hydrodynamic dispersion was introduced only in terms of a longitudinal dispersivity coefficient (α_{xx}) of 0.015 m, with transverse dispersion assumed negligible (i.e., $D_{yy}=D_{zz}=0$).

Permeant flow in the bioreactors was simulated with MODFLOW-2000 Version 1.7 (U.S. Geological Survey) as described in Harbaugh et al. (2000). Multispecies reactive transport was simulated with RT3D Version 2.5 (U.S. Department of Energy) as described in Clement (1997). RT3D transport was coupled to a user-defined subroutine containing the biochemical reaction kinetics in this research. In addition, the instantaneous-reaction algorithms [Eqs. (6) and (7)] were encoded into RT3D.

The model solution requires the simultaneous integration of all interdependent mass-balance equations of the system with respect to time. These equations include a nonlinear partial differential equation for each mobile species and a nonlinear ordinary differential equation for each immobile species. Numerical solution was obtained using reaction operator splitting, where the nonlinear ordinary differential equations (reactions) were solved by Runge-Kutta-Fehlberg integration. Transport time steps, which were on the order of 0.01 d, were selected on the basis of the requirements for advection, dispersion, and sink/source mixing automatically set in RT3D. Multiple time steps for Runge-Kutta

integration were required within each transport time step up to a total of 3,000 integration time steps, after which integration was stopped by the program.

The reactor was modeled as a prismatic, three-dimensional domain, containing nine rows, 61 columns (along the direction of flow), and one layer. The space discretization was 0.5 cm along rows and columns and 4.363 cm of layer height. Flow and transport boundary conditions were defined for one-dimensional flow and transport. Flow boundary conditions consisted of upper and lower specified hydraulic-head boundaries (Dirichlet) at column ends, with no-flow boundaries through each column side. Transport boundary conditions consisted of a specified concentration at the column input for species present in the influent solution and a zero dispersive mass-flux boundary (Neumann) at the end of the column (i.e., $x=L$). Initial conditions for species in the influent solution were $c(x,y,z,0)=0$ within domain cells. Organic materials and biomass initially present in the column were assigned initial conditions $c(x,y,z,0)\neq 0$. The RT3D run-times for typical simulations using either first-order or Contois kinetics were similar and on the order of 1/3 h.

Evaluation of Model Calibration

The quantitative evaluation of model calibration results involved assessing the magnitude of the sum of weighted squared errors (SWSE) resulting from the comparison between model-predicted concentrations (effluent) and measured values (experimental data) for effluent sulfate over observation times, as follows:

$$\mathrm{SWSE}=\frac{1}{(n-k)}\sum_{1}^{n} w_i\left(\frac{[c_{\mathrm{obs},i}]-[c_{\mathrm{sim},i}]}{[c_{\mathrm{obs},i}]}\right)^2 \tag{9}$$

where n=number of observations, $k=NP+1$ (where NP =number of model parameters), w_i=weight of observation i, and $[c_{\mathrm{obs},i}]$ and $[c_{\mathrm{sim},i}]$=respective observed and simulated effluent concentrations at the ith calibration time. By definition, observation weights w_i are calculated as equal to the inverse of the variance estimated as occurring in the measurement of observation i. For this study, the SWSE was programmed in MATLAB (MathWorks, Natick, Mass.).

Model Selection

As described in Poeter and Anderson (2005), the Akaike information criterion (AIC_C) was used for estimating expected Kullback-Leibler information, as follows:

$$\mathrm{AIC}_C=n\ \ln(\sigma^2)+2k+\frac{2k(k+1)}{n-k-1} \tag{10}$$

where σ^2=estimated residual variance, including a sum of weighted squared residuals, calculated on the basis of experimental data (observations) and modeled results, as follows:

$$\sigma^2=\frac{1}{n}\sum_{1}^{n} w_i([c_{\mathrm{obs},i}]-[c_{\mathrm{sim},i}])^2 \tag{11}$$

The second and third terms of Eq. (10) are first- and second-order bias terms resulting from a small number of observations ($n/k<40$). The weights w_i apply when the observation errors are independent and focus at placing more weight on data with less variance. Based on the assumption of measured concentrations with apparently an equal error, a single observation variance can be used for the entire experimental data set (i.e., w_i=const). For each model, a delta AIC_C value (Δ_i) and an Akaike weight of evidence ($w_{A,i}$) can be calculated, as follows:

$$\Delta_i=\mathrm{AIC}_{C,i}-\mathrm{AIC}_{C,\min} \tag{12}$$

$$w_{A,i}=\frac{e^{-0.5\Delta_i}}{\sum_{j=1}^{R} e^{-0.5\Delta_j}} \tag{13}$$

where R=total number of models being evaluated to select the one that minimizes information loss. Evidence ratios can be obtained as ratios of $w_{A,k}/w_{A,i}$, where k=best model in the sense described above, and i represents any other model in the model set.

Table 1. Water Quality for Samples Collected at NTA and SCA Sites and for Influent Solutions Fed to SR Biocolumns, i.e., after Limestone Pretreatments (Figueroa et al. 2007)

	NTA		SCA	
Chemical constituent	Collected water	Influent solution to biocolumns	Collected water	Influent solution to biocolumns
Sulfate, SO_4^{2-} (mg/L)	900	900	2,100	2,100
Zinc, Zn^{2+} (mg/L)	5–7	1–2	65–75	45–55
Ferrous iron, Fe^{2+} (mg/L)	40	<1	40	<1
Aluminum, Al^{3+} (mg/L)	<1	~0	<1	~0
pH	6.0–6.5	6.5	5.0–5.5	5.8

Biocolumn Experiments

Two pairs of duplicate treatment experiments were performed. The feed influent solutions used in the experiments were collected from two sites located in Colorado, viz. the National Tunnel Adit (NTA) and the Silver Cycle Mine Adit (SCA). The experiments were two-stage systems, with limestone pretreatment reactors for control of pH and Fe^{2+} and Al^{3+} removal followed by anaerobic SR biocolumns (see details in Figueroa et al. 2007). Water qualities for the samples collected at these sites (i.e., influent solutions for the two-stage treatments) and for the effluents from the limestone pretreatment (i.e., influent solutions for the SR biocolumns) are summarized in Table 1. As indicated in Table 1, the limestone pretreatment was aimed at removing excess Fe^{2+} and Al^{3+} to avoid the SR biocolumns from clogging, which can cause column failure before depletion of organic substrates.

The experimental data used for this study pertained specifically to SO_4^{2-} and Zn^{2+} effluent concentrations from the SR biocolumns. The anaerobic SR biocolumns consisted of 30-cm-long, 5.0-cm-diameter, acrylic tubes adapted with flanges with threaded influent and effluent fittings. Each biocolumn was packed with 17.0 g of corn stover and 194 g of fragmented walnut shells, both passing the 6.35-mm sieve, at equal volumes (i.e., 50% corn stover and 50% walnut shells mixture, by volume). No external inoculum for SR bacteria (e.g., manure) was employed.

Peristaltic pumps were used to generate flow rates from the bottom to the top of each biocolumn at either 60 mL/d of influent solution for the NTA biocolumns or 30 mL/d for the SCA biocolumns. After packing the biocolumns with the solid materials, an average of 433 mL was required to saturate each biocolumn with deionized water, resulting in a total porosity, n, of 0.73. Thus, the nominal solution residence times were 7.2 d in the NTA biocolumns and 14.4 d in the SCA biocolumns. Periodic sampling was performed to measure the outflow rate, pH, alkalinity, sulfate, and dissolved and total metals.

As shown in Table 1, a major difference between NTA and SCA biocolumns was the influent concentrations for Zn^{2+}. This difference is significant, since zinc has been reported to have inhibitory effects on the growth of sulfate reducers above 25–50 mg/L (Utgikar et al. 2003), and cellulolytic fermenters above 1 mg/L free zinc concentration (Ruhs et al. 2006).

Sulfate concentrations were calculated directly from the total measured sulfur in aqueous solution. Total sulfur and metals were analyzed by inductively coupled plasma-absorbance emission spectroscopy (ICP-AES) (Perkin Elmer Optima 3000). Samples were filtered through 0.45-μm syringe-tip filters, diluted with Milli-Q water, and acidified to pH 2 with trace metals-grade nitric acid (Mallinckrodt). The detection limits were 0.05 mg/L and 0.002 mg/L for sulfur and zinc, respectively. Values of pH were measured using an Orion 910500 probe and Series 200 meter (Denver Instruments, Arvada, Colo.). Organic compositions of the corn stover and walnut shells were determined by Venot (2008) using hot water (TAPPI 1999) and acid extractions (Templeton and Ehrman 1995) coupled with total dry weight (sample dried at 103°C) and organic content measurement, by the difference between total dry weight and fixed solids dried at 550°C.

NTA Biocolumns

As shown in Fig. 2(a), the measured effluent solution pH for the NTA duplicate biocolumns (NTA-1 and NTA-2) indicated similar trends, with pH values being lower than 5 at the onset of the experiments and lower than 6 for pore volumes of flow, PVF ($=vt/L$, where v=constant seepage velocity, t=time, and L =column length), <5.5, and subsequently increasing to 6.5 and 7.5 at ~10 and ~16 PVF, respectively. The early-time pH that generally was lower than that of the influent solution coming from the limestone pretreatment (6.0–6.5) may be indicative of material leaching. Subsequently, the increasing effluent pH occurring in both columns may be attributed to alkalinity production by sulfate reduction.

As shown in Fig. 2(b), effluent sulfate concentrations were approximately stabilized between ~500 and 600 mg/L at ~15 PVF, which is below the concentration level of the influent solution supplied to the columns (900 mg/L). Sulfate removal after 30 d (4.3 PVF) stabilized at an average rate of sulfate reduction of ~0.28 mmol S/L d^{-1}. As shown in Fig. 2(c), removal of zinc to <0.1 mg/L occurred for both NTA biocolumns within approximately 21 d (3 PVF).

SCA Biocolumns

Compared to the NTA duplicate columns, the pair of SCA biocolumns (SCA-1 and SCA-2) was tested under double the solution residence time, albeit with significantly higher $[Zn^{2+}]$ in the influent solution. The experimental results from the pair of SCA biocolumns were distinct. As shown in Fig. 3(a), measured effluent pH for SCA-1 increased from 5 to 5.5 (PVF<2) to 7.0

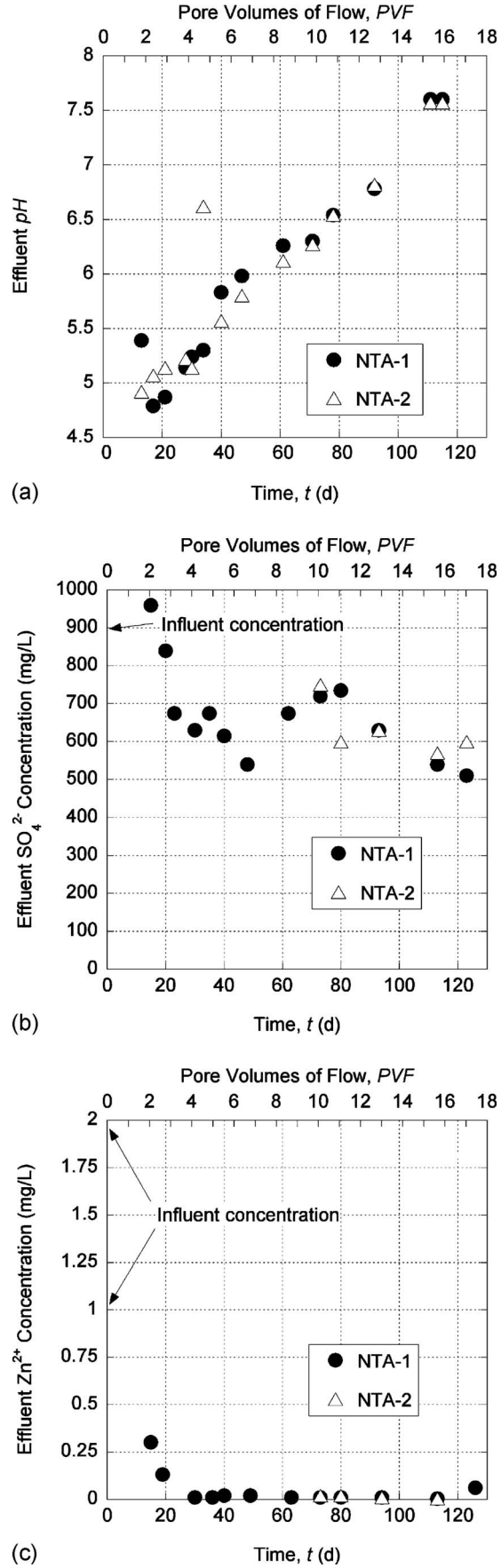

Fig. 2. Experimental effluent data for duplicate NTA biocolumns NTA-1 and NTA-2: (a) pH; (b) sulfate; (c) zinc

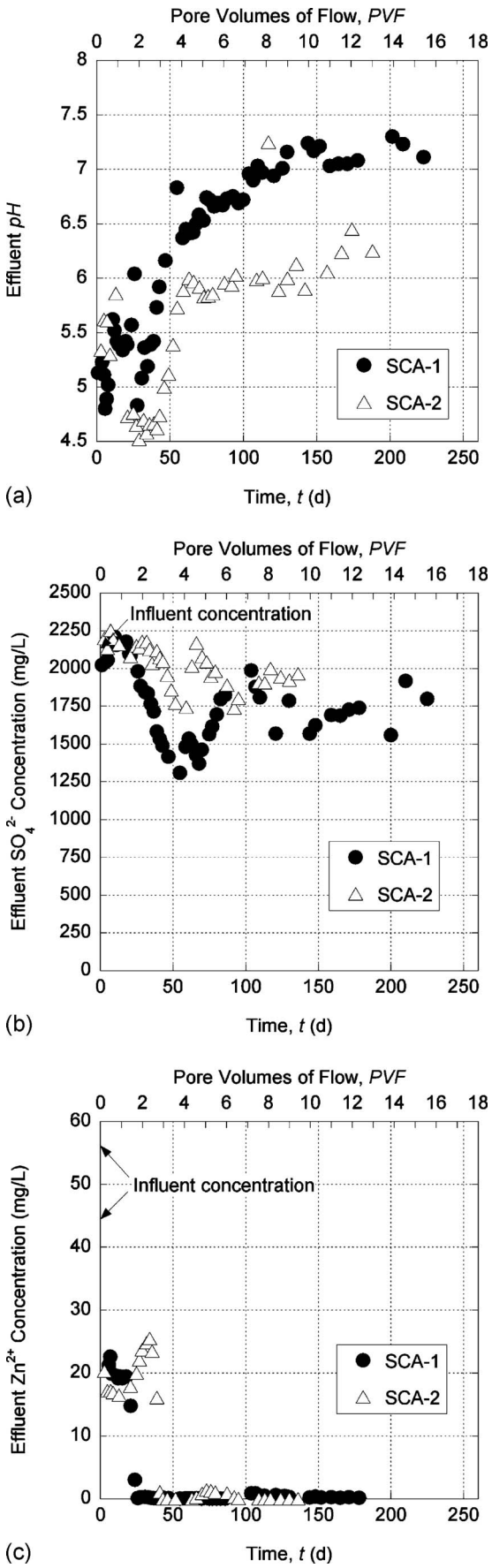

Fig. 3. Experimental effluent data for duplicate SCA biocolumns SCA-1 and SCA-2: (a) pH; (b) sulfate; (c) zinc

$\leq$pH$\leq$7.5 for PVF$>$7 to 8. In contrast, effluent pH for SCA-2 remained at significantly lower levels, both near the onset of the experiment (4.5$\leq$pH$\leq$5, for PVF$\approx$2–3) and in the longer term (pH$\approx$6 for 5$\leq$PVF$\leq$end of test). Therefore, the SCA-2 failed during the test.

Possible explanations for the distinct results include the fact that the SCA biocolumns were under more stress due to higher $[Zn^{2+}]$ than were the NTA biocolumns, as well as the possibility of experimental error in the case of the failure of SCA-2. For example, there was a 30-d lag in the startup of the SCA-2, with differences in temperature and flow conditions during the initial period of the test. In addition, a 10-d loss of flow occurred at early times for the SCA-2, which may have resulted in depletion of sulfate and a synergistic community of fermenters, acidogens, and methanogens developing, thereby hindering the development of full sulfate reduction in this column. The results shown in Figs. 3(b and c) corroborate the poorer performance of SCA-2.

As shown in Fig. 3(b), effluent sulfate concentrations varied more widely than those for the NTA experiments, but approximately stabilized at $\sim$1,750 mg/L at $\sim$12 PVF for SCA-1. Sulfate removal after 50 d (3.6 PVF) stabilized at an average rate of sulfate reduction of $\sim$0.29 mmol S/L d^{-1}, similar to that of the NTA biocolumns. As shown in Fig. 3(c), the removal of zinc to $<$0.1 mg/l occurred for both SCA biocolumns within approximately 2 PVF for SCA-1. Based on the pH and $[SO_4^{2-}]$ trends described above, SCA-2 was considered to have failed and the data were disregarded.

Solid Substrates

The initial amounts of solid decomposable material (polysaccharide, g/L) in a given biocolumn were not explicitly known, but were not simply equal to the total dry mass of packed organic materials. Fractions such as lignin ($\sim$25–35%, by dry mass, in woods, 15–20% in leaves and grass), protected/recalcitrant polysaccharide tissues ($\sim$15–20%), and water soluble organics and inorganics ($\sim$5% in woods, 15–25% in leaves and grass) were discounted due to significantly lower rates of degradation of these solids and washout of the water soluble components (e.g., Sylvia et al. 1998). For the corn-stover material utilized in this research, the fractions of lignin and water soluble organics were determined to be 15 and 16%, respectively (Venot 2008).

Combining representative percentages, a 50% degradable polysaccharide fraction (dry-mass basis) was considered for the corn stover. Estimates of lignocellulosic material biodegradability by the methods of Chandler et al. (1980) and Van Soest (1994) using the corn-stover composition reported by Venot (2008) were 40 and 60%, respectively. Thus, the 17 g of packed corn stover were simulated as 20 g/L of initial decomposable polysaccharides. Walnut shells, which are far less degradable than corn stover, represented the structural granular medium in the biocolumns. The decomposable polysaccharides were assumed as $\sim$10% on a dry-mass basis, which is consistent with the degradable fraction estimated using the method by Van Soest (1994) for a holocellulose to lignin ratio of 1.5. Thus, the 194 g of packed material were simulated as 40 g/L of initial decomposable polysaccharides.

Previous Parameter Values

The previous study by Hemsi et al. (2005) focused on approximating experimental rates of sulfate reduction at 25°C in batch

Table 2. Decomposition Rate Equations, Adjustable and Tied Parameters, and Initial Concentration Values Employed in Models F1–F3 and C1–C3

Model	s	Decomposition rate equations ($i=1\ldots s$)	Parameters: Adjustable	Parameters: Tied	Initial concentration (g/L)
F1	1		$k_{f,1}$	—	$[CE_1]=20$ $[LA]=0$
F2	2	$\frac{d[CE_i]}{dt}=-k_{f,i}[CE_i]$ $\frac{d[LA]}{dt}=Y_{LA/CE}\sum_i\left(-\frac{d[CE_i]}{dt}\right)$	$k_{f,1}$	$k_{f,2}=0.1\ k_{f,1}$	$[CE_1]=20$ $[CE_2]=40$ $[LA]=0$
F3	3		$k_{f,1}$	$k_{f,2}=0.1\ k_{f,1}$ $k_{f,3}=10\ k_{f,1}$	$[CE_1]=20$ $[CE_2]=40$ $[CE_3]=4$ $[LA]=0$
C1	1		$k_{c,1}$ $K_{A,1}$	$d_1=0.1\ k_{c,1}$	$[CE_1]=20$ $[X_{d,1}]=0.1$ $[LA]=0$
C2	2	$\frac{d[CE_i]}{dt}=-k_{c,i}[X_{d,i}]\left(\frac{[CE_i]/[X_{d,i}]}{K_{A,i}+[CE_i]/[X_{d,i}]}\right)$ $\frac{d[X_{d,i}]}{dt}=Y_{Xd,CE}\left(-\frac{d[CE_i]}{dt}\right)-d_i[X_{d,i}]$	$k_{c,1}$ $K_{A,1}$	$k_{c,2}=0.1\ k_{c,1}$ $K_{A,2}=K_{A,1}$ $d_1=0.1\ k_{c,1}$ $d_2=0.1\ k_{c,2}$	$[CE_1]=20$ $[CE_2]=40$ $[X_{d,1}]=0.1$ $[X_{d,2}]=0.2$ $[LA]=0$
C3	3	$\frac{d[LA]}{dt}=Y_{LA/CE}\sum_i\left(-\frac{d[CE_i]}{dt}\right)$	$k_{c,1}$ $K_{A,1}$	$k_{c,2}=0.1\ k_{c,1}$ $k_{c,3}=10\ k_{c,1}$ $K_{A,2}=K_{A,1}$ $K_{A,3}=K_{A,1}$ $d_1=0.1\ k_{c,1}$ $d_2=0.1\ k_{c,2}$ $d_3=0.1\ k_{c,3}$	$[CE_1]=20$ $[CE_2]=40$ $[CE_3]=4$ $[X_{d,1}]=0.1$ $[X_{d,2}]=0.2$ $[X_{d,3}]=0.02$ $[LA]=0$

Note: s=number of substrates; $Y_{LA/CE}=0.859$ g/g; $Y_{Xd/CE}=0.181$ g/g; and initial ratio $[X_{d,i}]/[CE_i]=0.005$.

experiments based on solid decomposable substrates. For pure cellulose, a first-order hydrolysis rate coefficient, k_f, of 0.005 d^{-1} was obtained. In terms of Contois kinetics for cellulose, $k_c=0.625$ d^{-1} and $K_A=37$ g/g. For wood chips, leaf mulch, and sawdust, the values for k_c were 0.4, 0.625, and 0.8 d^{-1}, respectively, with $K_A=30$ g/g. Vavilin et al. (2004) modeled cellulose hydrolysis at 35°C using Contois kinetics, with $k_c=1.25$ d^{-1} and $K_A=7.5$ g/g, which is consistent with the values reported in Hemsi et al. (2005), i.e., taking into account the difference in temperature.

Results

Experimental results in terms of sulfate removal rates ranged between 0.1 and 0.3 mmol S/L d^{-1}, which were within the range from 0.1 to 2 mmol S/L d^{-1} observed in laboratory and field studies (Wildeman et al. 1997; Waybrant et al. 1998; Neculita et al. 2007). Tuttle et al. (1969) reported rates from ~0.1 to 0.2 mmol S/L d^{-1} for wood-dust SR biocolumns for AMD remediation tested at 22°C.

Model Calibration

The different models proposed are shown in Table 2. The definition of Models F1–F3 and C1–C3 is aimed at investigating the effects of the type of kinetics used for solid-substrate hydrolysis (F≡first-order versus C≡Contois) and the number of pools of decomposable materials considered. Each model was calibrated by minimizing the calibration error (SWSE) between simulated and experimental NTA-1 effluent concentrations for SO_4^{2-} versus time (Tables 3 and 4). Rates of sulfate reduction, effluent concentrations for Zn^{2+}, and the final dry mass of solid organic material were compared in the figures.

Inverse modeling (e.g., Poeter and Hill 1997) was not employed in this study. The optimization routine for searching

Table 3. SWSE Values Obtained during Calibration of First-Order Models F1–F3 as a Function of Tested $k_{f,1}$ Values

First-order models	$k_{f,1}$ (d^{-1})	SWSE (10^{-5})
F1	3×10^{-3}	5.56
	4×10^{-3}	4.41
	4.5×10^{-3}	4.09
	5×10^{-3}	3.92
	6×10^{-3}	3.94
	7×10^{-3}	4.36
F2 ($k_{f,2}=0.1\ k_{f,1}$)	3×10^{-3}	4.13
	4×10^{-3}	3.14
	4.5×10^{-3}	2.99
	5×10^{-3}	3.03
	6×10^{-3}	3.63
	7×10^{-3}	4.78
F3 ($k_{f,2}=0.1\ k_{f,1}$) ($k_{f,3}=10\ k_{f,1}$)	1×10^{-3}	6.51
	2×10^{-3}	4.90
	2.5×10^{-3}	4.96
	3×10^{-3}	5.32
	4×10^{-3}	6.61
	5×10^{-3}	8.33

Note: $k_{f,i}$=first-order decomposition rate coefficient for substrate i and $w_i=0.0016$ $(mg/L)^{-2}$ [Eq. (9)].

Table 4. SWSE Values Obtained during Calibration of Contois Models C1–C3 as a Function of Tested $k_{c,1}$ and $K_{A,1}$ Values

		$K_{A,1}$ (g/g)			
		7.5	15	30	60
Contois models	$k_{c,1}$ (d^{-1})	SWSE (10^{-5})			
C1	0.2	4.69	6.67	8.99	11.2
	0.3	1.29	2.50	5.37	8.61
	0.4	2.15	1.30	3.12	6.53
	0.5	8.49	2.51	2.16	4.99
	0.6	20.2	5.49	2.30	3.96
C2 ($k_{c,2}$=0.1 $k_{c,1}$)	0.2	4.05	5.93	8.20	10.5
	0.3	1.17	1.92	4.49	7.63
	0.4	2.63	1.15	2.33	5.43
	0.5	9.22	2.88	1.64	3.86
	0.6	21.3	6.83	2.15	2.90
C3 ($k_{c,2}$=0.1 $k_{c,1}$) ($k_{c,3}$=10 $k_{c,1}$)	0.2	8.05	6.13	5.69	6.48
	0.3	8.43	6.44	5.35	5.39
	0.4	6.16	6.77	5.83	5.19
	0.5	10.7	7.74	6.77	5.49
	0.6	22.0	10.6	8.14	6.15

Note: $k_{c,i}$=Contois decomposition rate coefficient for substrate i; $K_{A,i}$ =Contois affinity coefficient for substrate i; w_i=0.0016 $(mg/L)^{-2}$ [Eq. (9)].

SWSE minima was simply based on picking parameter values from lists defined based on predefined ranges of variation. Given the input parameter values, the model was tested and the SWSE calculated [Eq. (9)]. Resulting SWSE values were inspected and ranges were reset if a minimum SWSE was not found. Final ranges for the kinetic coefficients for corn stover were $0.001 \leq k_f \leq 0.007$ d^{-1} for first-order models, and $0.1 \leq k_c \leq 0.6$ d^{-1} and $7.5 \leq K_A \leq 60$ g/g for Contois models (Tables 3 and 4).

Due to the limited number of observations in the NTA-1 sulfate data set (n=13), the number of adjustable parameters was limited for parsimony. Models with two or more material pools were subject to parameter tying, whereby decomposition parameters for materials other than corn stover were tied to corn-stover parameters (Table 2). Also, the first-order decay coefficient for biomass d_i [Eq. (3)] was tied to $k_{c,i}$ as shown in Table 2. By imposing parameter tying, first-order models with k=2 (n/k =6.5) and Contois models with k=3 (n/k=4.3) were defined. These n/k ratios denote calibration under small-sample conditions, corresponding to $n/k<40$ (Burnham and Anderson 2004). Thus, doubling or tripling the number of parameters in the models appeared unsuitable given the limitations in the available data set. Following calibration, models were compared using a formal model comparison metric (Poeter and Anderson 2005).

For calibration and model ranking, observed concentrations were assumed to have been measured with an equal error, and a single value for observation weight, w_i, was used [Eqs. (9) and (11)]. The value 0.0016 $(mg/L)^{-2}$ was calculated based on the assumption that concentrations were determined with 95% confidence within ±5%.

Effect of Type of Kinetic Model

The different models proposed for this study include first-order (F1–F3) and Contois (C1–C3) models (Table 2). For each model, a minimum value of SWSE was obtained after testing the model against the experimental data for different values of model parameters, i.e., k_f for first-order models and k_c and K_A for Contois models. The results for SWSE are shown in Tables 3 and 4 for first-order and Contois models, respectively, with calibrated models having SWSE values ranging from ~3 to 5×10^{-5} for first-order models and from ~1 to 5×10^{-5} for Contois models.

Table 5. Model Ranking for Models F1–F3 and C1–C3 Using the Akaike Information Criterion [Eqs. (10)–(13)]

Model designation	Model ranking results					
	NP	k	AIC_C	Δ_i	$w_{A,i}$	$w_{A,C2}/w_{A,i}$
F1	1	2	36.4	11.1	0.002	260
F2	1	2	34.8	9.5	0.005	115
F3	1	2	39.8	14.4	0.0005	1,300
C1	2	3	26.5	1.2	0.4	1.8
C2	2	3	25.3	0	0.6	1.0
C3	2	3	44.8	19.5	0.00004	17,000

Note: NP=number of model adjustable parameters; $k=NP+1$; AIC_C =Akaike information criterion value; Δ_i=delta AIC_C value for model i; $w_{A,i}$=Akaike weight of evidence for model i; $w_{A,C2}/w_{A,i}$=weight of evidence ratios relative to Model C2; number of observations in NTA-1 data set, n=13.

Contois models were observed, in general, to adhere more closely to the experimental data points than first-order models as denoted by the resulting lower SWSE values. Eq. (9) includes $(n-k)$ in the denominator accounting for the difference in number of model parameters between the models. As shown in Table 5, AIC_C, Δ_i, Akaike weight of evidence [Eqs. (10), (12), and (13)], and evidence ratios were calculated for each of the calibrated proposed models. The results indicated that the proposed C2 and C1 model hypotheses were supported to a greater extent by the data, since for these models the lowest AIC_C values of 25.3 and 26.5 were obtained. For first-order models F1–F3, the AIC_C values ranged from ~35 to 40.

Effect of Number of Pools of Decomposable Materials

As previously described, models with a single pool of decomposable materials were designed to contain the equivalent of a 20-g/L initial concentration of decomposable polysaccharides in only corn stover. Dual-substrate models included an initial 20 and 40 g/L of decomposable polysaccharides in the corn stover and fragmented walnut shells. The triple-pool models included a third pool of a more easily degradable, nearly soluble saccharide at an initial concentration of 4 g/L (Table 2). During model calibration, within each group of proposed models (first-order versus Contois), the lowest values of SWSE were obtained when calibrating the dual-substrate Models F2 and C2, with calibrated dual-substrate models having SWSE values of 2.99×10^{-5} for Model F2 and 1.15×10^{-5} for Model C2. In addition, the value of SWSE for the single-substrate Model C1 was 1.29×10^{-5}.

Also, within each group of models (first-order versus Contois), the lowest values of AIC_C were obtained for dual-substrate models (F2 and C2). Although Model F2 was the best of the first-order models considered in this study, Models C2 and C1 were superior to Model F2 by a considerable amount, as denoted by Model F2 having a Δ_i value of 9.5 (with respect to the best model in the set, i.e., Model C2) compared to the value of 1.2 for Model C1. As discussed in Poeter and Anderson (2005), relative to the best model in the set, models with $\Delta_i<2$ are very good models, whereas models with $4<\Delta_i<7$ have less empirical support. In most cases, models with $\Delta_i>\sim10$ can be dismissed from further consideration.

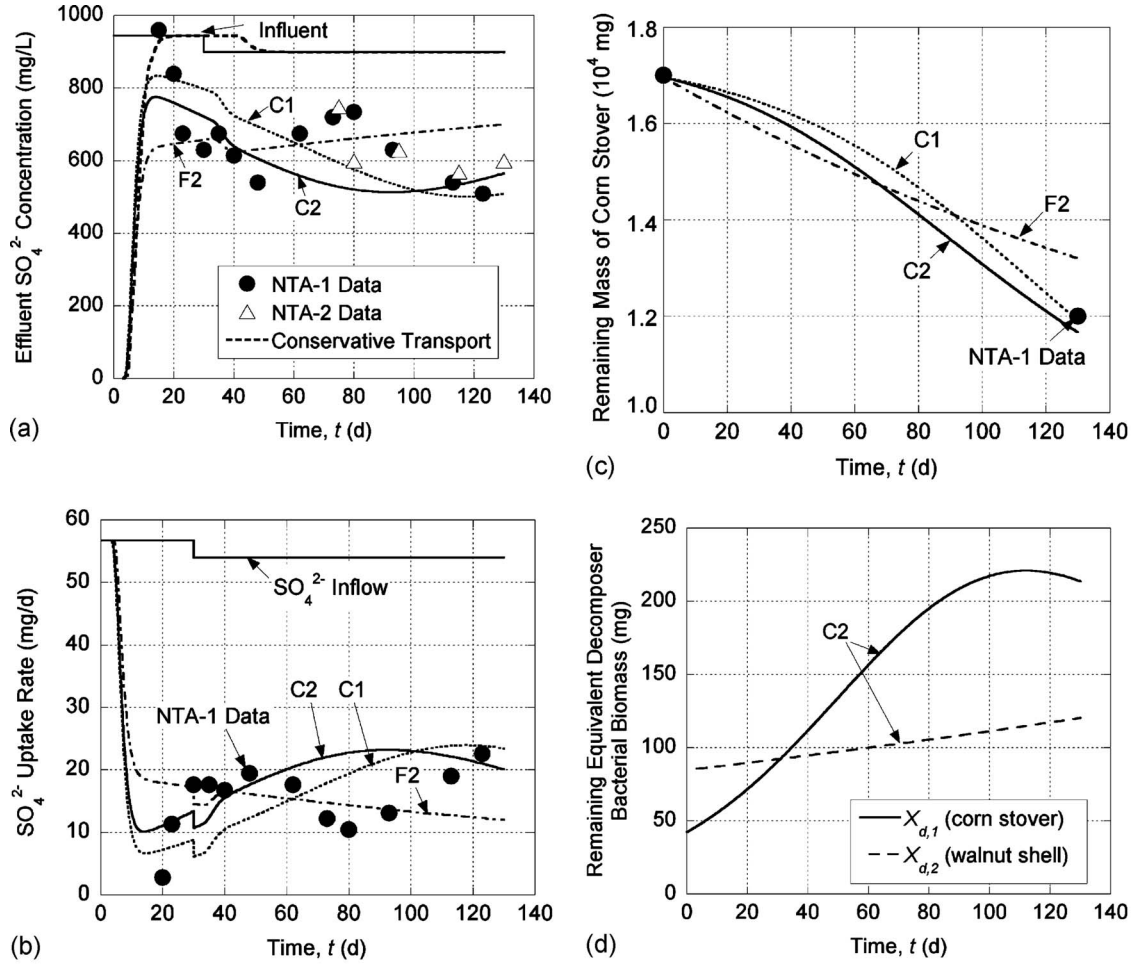

Fig. 4. Results from model calibration using NTA-1 data considering first-order Model F2 and Contois Models C1 and C2 compared to experimental data: (a) effluent sulfate; (b) rates of sulfate uptake; (c) total remaining mass of corn stover; (d) modeled total equivalent biomass of decomposers for Model C2

Effect of Initial Biomass of Decomposer Bacteria

Additional simulations performed using the C2 Contois model as shown in Table 2, but with different values for the initial biomass population of decomposer bacteria assumed for simulation, were performed and SWSE values were obtained. As shown in Table 2, the initial value for $[X_d]/[CE]$ of 0.005 was considered in this study, as previously tested by Hemsi et al. (2005). The effect of the initial biomass of decomposer bacteria was evaluated by performing simulations with values for $[X_d]/[CE]$ that differed from the previous value by a factor of 10 (i.e., 0.0005 and 0.05). For the assumptions considered in the Contois models shown in Table 2, the lowest values of SWSE were obtained for the initial value for $[X_d]/[CE]$ of 0.005.

Simulated trends for effluent concentrations of SO_4^{2-} and rates of sulfate uptake, and total remaining equivalent concentration of solid substrates, versus time are compared to the measured experimental data in Figs. 4(a–c). Three models are shown in these figures, i.e., Models F2, C1, and C2, whereas Models C1 and C2 were the best of the proposed models, as shown in Table 5.

In Fig. 4(a), the simulated results for Model F2 differ from the results obtained with Contois Models C1 and C2 in that Model F2 displays the lowest early-time effluent SO_4^{2-} concentrations. As shown in Fig. 4(b), the time rate of sulfate reduction with Model F2 is a maximum at the beginning of the simulation and declines monotonically with time as the solid substrate is consumed, as previously observed for simulation of sulfate reduction in solid-substrate batch tests (Hemsi et al. 2005). Comparing effluent SO_4^{2-} modeled by C1 and C2, Model C2 presents higher rates of sulfate reduction [Fig. 4(b)] than Model C1 due possibly to some combination of the effects of having higher k_c for the corn stover (i.e., 0.4 d^{-1} versus 0.3 d^{-1} in Model C1) and containing the walnut substrate. The ability to explain the results in terms of k_c values is somewhat complicated by the differences in K_A in these models (15 g/g versus 7.5 g/g). However, for times >105 d, the rate of sulfate reduction predicted by Model C1 surpasses that of Model C2, despite the effect of the presence of walnut shells. This observation suggests that, for the parameter tying assumptions considered, the most impacting substrate was corn stover. Simulated effluent concentrations for Zn^{2+} for the test duration of <130 d remained approximately zero for Models F2, C1, and C2, in agreement with the data shown in Fig. 2(c).

The experimental data provided for the comparison shown in Fig. 4(c) are based on the measured variation in the total dry mass of solid substrate per bioreactor (average) after 130 d of 5.0 g. As shown in Fig. 4(c), Models C1 and C2 resulted in good simulations of the measured mass variation in solid organic substrate, assuming that walnut shell mass variation was negligible. Decom-

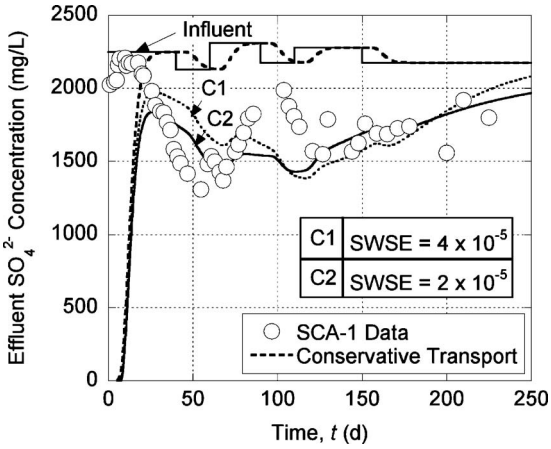

Fig. 5. Model verification with SCA-1 data considering Models C1 and C2

poser bacteria biomass versus time is shown in Fig. 4(d) for Model C2, i.e., for decomposers associated with corn-stover and walnut-shell substrates.

Model Testing

Models C2 and C1, which resulted in the lowest AIC_C values in model ranking based on experimental data from NTA-1, were subsequently used in attempts to model the experimental results of an independent test, SCA biocolumn 1 (i.e., SCA-1). As shown in Fig. 5, model simulations of effluent SO_4^{2-} concentrations versus time compare well to experimental data (i.e., measured effluent SO_4^{2-} in SCA-1 versus time), for calibrated Models C2 and C1. The computed values of SWSE for these simulations with respect to the SCA-1 data (Fig. 5) are 2.1×10^{-5} for Model C2 and 4.0×10^{-5} for Model C1, assuming $w_i=0.0016$ $(\mathrm{mg/L})^{-2}$, as assumed for the previous calibrations. Therefore, Model C2, which was the best model among the proposed models in this study for simulating NTA-1 data, also was the best model for simulating experimental data from the independent SCA-1 experiment. One factor to bear in mind in terms of the SCA-1 data is that the possible biological inhibition due to Zn^{2+} was not considered in the models, but may have occurred in SCA-1 due to the reasons previously explained.

Model Prediction: Longevity of NTA-1

Assessments of longevity for biological passive treatment systems are widely recognized as a major issue related to design and operation. Modeling was applied in attempting to predict longer-term behavior (i.e., beyond the testing time of 130 d) for the NTA-1 biocolumn, considering the best calibrated models in this study, Models C2 and C1. The longer-term behavior of NTA-1 was modeled considering a total time of 730 d (2 yr).

As shown in Fig. 6(a), effluent SO_4^{2-} concentrations were predicted to increase and approach influent concentrations after ~300 d of biocolumn operation for Model C1 and to remain slightly less than influent concentration (~850 mg/L) for Model C2. This time is interpreted, for both models, as being associated with the end of decomposition of degradable polysaccharides in corn stover as shown in Fig. 6(b). The models also predicted the remaining mass of degradable polysaccharides in corn stover to be depleted and the associated bacterial population (equivalent

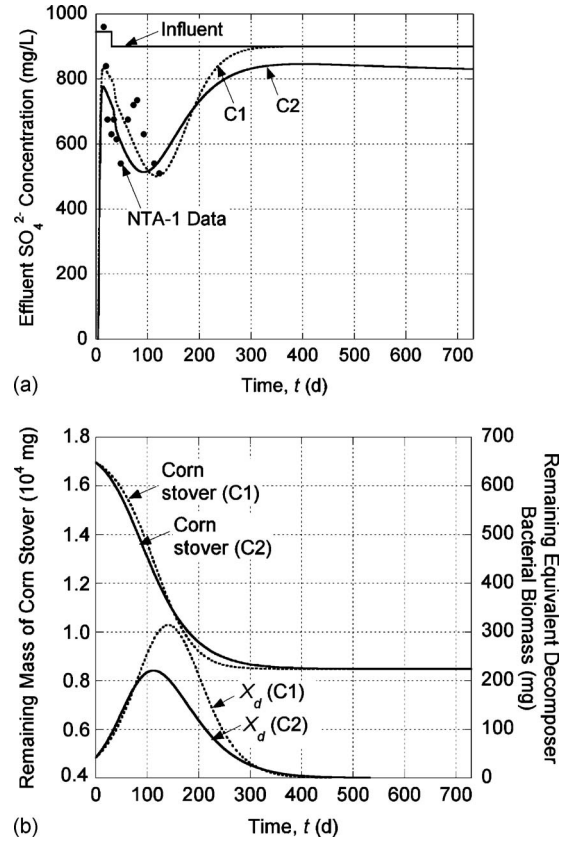

Fig. 6. Model (C1 and C2) predictions for NTA-1: (a) longer-term effluent sulfate concentrations; (b) decomposable polysaccharides and decomposer bacteria

biomass concentration) to decline reaching zero at ~400 d. This predicted biocolumn longevity is a function of the small particle size of the corn stover and the limited amount of bioavailable substrate. Increased operational life in a field implementation will require the modification of the substrate mixture to include a larger fraction of bioavailable substrate and also should include larger particles to decrease the overall rate of organic substrate decomposition.

Conclusions

New reactive transport models for the bioremediation of mining influenced waters in solid-phase bioreactors were calibrated against experimental data, tested for an independent data set, and employed for predictions of biocolumn longevity beyond testing time. First-order (F) and Contois (C) kinetics for decomposition as well as different numbers of pools of decomposable materials were proposed in different models (F1–F3 and C1–C3). Calibrations were quantified by assessing calibration error SWSE on the basis of model predictions of biocolumn effluent concentrations for SO_4^{2-} against data from Column NTA-1. Due to limitations in the calibration data set, the number of adjustable model parameters was limited using parameter tying. Calibrated models were ranked using the Akaike information criterion (AIC_C).

Models based on Contois kinetics with initial population of decomposer bacteria corresponding to $[X_d]/[CE]=0.005$ and kinetic parameters for decomposition of corn stover $k_c=0.4$ d^{-1} and $K_A=15$ g/g (Model C2, with tied parameters for walnut shells)

and $k_c=0.3\ \mathrm{d}^{-1}$ and $K_A=7.5\ \mathrm{g/g}$ (Model C1) attained the lowest values of AIC_C. Thus, Models C2 and C1 (i.e., based on Contois kinetics) emerged as the models that were supported to a greater extent by the data. As a result, model testing was performed for the independent SCA-1 biocolumn data considering only Models C2 and C1 and parameter values from calibration (NTA columns). Comparisons of the modeling and experimental results indicated good approximations of effluent sulfate, with overall discrepancy (SWSE) within the range of calibration errors obtained for the calibration data sets.

Finally, model prediction of biocolumn longevity was performed on the calibration data set (NTA-1). The predicted performance indicated that the experiment would have remained operative, i.e., before depleting the SR capacity, for an additional ~200 d after termination of the biocolumns in the laboratory. Future model validation using longer-term field data sets will be necessary to confirm model predictions.

Acknowledgments

This research was funded by the U.S. EPA Science to Achieve Results (STAR) Program under Grant No. R-82951501-0 as part of the U.S. EPA's Rocky Mountain Regional Hazardous Substance Research Center. The writers are grateful to Dr. E. Poeter for assistance on the application of multimodel ranking.

References

Batstone, D. J., et al. (2002). "The IWA anaerobic digestion model No. 1 (ADM1)." *Water Sci. Technol.*, 45(10), 65–73.

Bechard, G., Yamazaki, H., Gould, W. D., and Bedard, P. (1994). "Use of cellulosic substrates for the microbial treatment of acid mine drainage." *J. Environ. Qual.*, 23(1), 111–116.

Benner, S. G., Blowes, D. W., Gould, W. D., Herbert, R. B., and Ptacek, C. J. (1999). "Geochemistry of a permeable reactive barrier for metals and acid mine drainage." *Environ. Sci. Technol.*, 33(16), 2793–2799.

Burnham, K. P., and Anderson, D. R. (2004). "Multimodel inference: Understanding AIC and BIC model selection." *Sociolog. Methods Res.*, 33(2), 261–304.

Chandler, J. A., Jewell, W., Gossett, J., Van Soest, P., and Robertson, J. (1980). "Predicting methane fermentation biodegradability." *Biotechnol. Bioeng. Symp.*, 10, 93–107.

Chang, I. S., Shin, P. K., and Kim, B. H. (2000). "Biological treatment of acid mine drainage under sulphate-reducing conditions with solid waste materials as substrates." *Water Res.*, 34(4), 1269–1277.

Chynoweth, D. P., and Pullammanappallil, P. (1996). "Anaerobic digestion of municipal solid waste." *Microbiology of solid waste*, A. Palmasano and M. Barlaz, eds., CRC, Boca Raton, Fla., 77–113.

Clement, T. P. (1997). *A modular computer code for simulating reactive multispecies transport in 3-dimensional groundwater systems RT3D Version 1.0*, U.S. Dept. of Energy and Pacific Northwest National Laboratory, PNNL-11720-1997.

Colberg, P. J. (1988). "Anaerobic microbial degradation of cellulose, lignin, oligolignols and monoaromatic lignin derivatives." *Biology of anaerobic microorganisms*, A. J. B. Zehnder, ed., Wiley-Liss, New York, 42–47.

Contois, D. E. (1959). "Kinetics of bacterial growth, relationship between population density and specific growth rate of continuous cultures." *J. Gen. Microbiol.*, 21(1), 40–50.

Drury, J. W. (2000). "Modeling of sulfate reduction in anaerobic solid substrate bioreactors for mine drainage treatment." *Mine Water and the Environment*, 19(1), 19–29.

Dvorak, D. H., Hedin, R. S., Edenborn, H. M., and McIntire, P. E. (1992). "Treatment of metal-contaminated water using bacterial sulfate reduction: Results from pilot-scale reactors." *Biotechnol. Bioeng.*, 40(5), 609–616.

Figueroa, L., Miller, A., Zaluski, M., and Bless, D. (2007). "Evaluation of a two-stage passive treatment approach for mining influenced waters." *2007 National Meeting of the American Society of Mining and Reclamation*, R. I. Barnhisel, ed., American Society of Mining and Reclamation, Gillette, Wyo.

Gibert, O., de Pablo, J., Cortina, J. L., and Ayora, C. (2004). "Chemical characterization of natural organic substrates for biological mitigation of acid mine drainage." *Water Res.*, 38(19), 4186–4196.

Groudev, S., Nicolova, M., Spasova, I., and Schutte, R. (2003). "Treatment of waters from a copper mine by means of a permeable reactive barrier." *Fifty years of the University of Mining and Geology "St. Ivan Rilski,"* Vol. 46, Univ. of Mining and Geology, Sofia, Bulgaria, 229–231.

Hallberg, K., and Johnson, D. (2005). "Microbiology of a wetland ecosystem constructed to remediate mine drainage from a heavy metal mine." *Sci. Total Environ.*, 338(1–2), 53–66.

Hammack, R. W., and Edenborn, H. M. (1992). "The removal of nickel from mine waters using bacterial sulfate reduction." *Appl. Microbiol. Biotechnol.*, 37(5), 674–678.

Harbaugh, A. W., Banta, E. R., Hill, M. C., and McDonald, M. G. (2000). "MODFLOW-2000, the U.S. Geological Survey modular groundwater model—User guide to modularization concepts and the groundwater flow process." *USGS Open-File Rep. No. 00-92*, U.S. Department of Interior and USGS, Reston, Va.

Hemsi, P. S., Shackelford, C. D., and Figueroa, L. A. (2005). "Modeling the influence of decomposing organic solids on sulfate reduction rates for iron precipitation." *Environ. Sci. Technol.*, 39(9), 3215–3225.

Henze, M., Gujer, W., and Mino, T., eds. (2000). "Activated sludge models ASM1, ASM2, ASM2D and ASM3." *Scientific and Technical Rep. No. 9*, IWA, Alliance House, London.

Humphrey, A. E. (1979). "The hydrolysis of cellulosic materials to useful products." *Hydrolysis of cellulose: Mechanisms of enzymatic and acid catalysis*, Advances in Chemistry Series, Vol. 181, American Chemical Society, Washington, D.C., 2, 25–53.

Mayer, K. U., Frind, E. O., and Blowes, D. W. (2002). "Multicomponent reactive transport modeling in variably saturated porous media using a generalized formulation for kinetically controlled reactions." *Water Resour. Res.*, 38(9), 1–21.

Monod, J. (1949). "The growth of bacterial cultures." *Annu. Rev. Microbiol.*, 3, 371–394.

Neculita, C. M., Zagury, G. J., and Bussière, B. (2007). "Passive treatment of acid mine drainage in bioreactors using sulfate-reducing bacteria: Critical review and research needs." *J. Environ. Qual.*, 36(1), 1–16.

Place, D., Figueroa, L., Wildeman, T., and Reisman, D. (2006). "Characterizing and tracking reactive mixture alterations: New tools for passive treatment system design and monitoring." *Proc., 7th Int. Conf. on Acid Rock Drainage*, R. I. Barnhisel, ed., Am. Soc. Mining and Reclamation (ASMR), Lexington, Ky., 1605–1619.

Poeter, E. P., and Anderson, D. R. (2005). "Multimodel ranking and inference in groundwater modeling." *Ground Water*, 43(4), 597–605.

Poeter, E. P., and Hill, M. C. (1997). "Inverse models: A necessary next step in groundwater models." *Ground Water*, 35(2), 250–260.

Prommer, H., Barry, D. A., Chiang, W. H., and Zheng, C. (2001). "PHT3D—A MODFLOW/MT3DMS-based reactive multicomponent transport model." *MODFLOW 2001 and other modeling odysseys*, H. Seo, E. Poeter, and C. Zheng, eds., International Ground-Water Modeling Center, Colorado School of Mines, Golden, Colo., 477–483.

Pruden, A., Pereyra, L., Hiibel, S., Inman, L., Kashani, N., Reardon, K., and Reisman, D. (2006). "Microbiology of sulfate reducing passive treatment systems." *Proc., 7th Int. Conf. on Acid Rock Drainage*, R. I. Barnhisel, ed., Am. Soc. Mining and Reclamation (ASMR), Lexington, Ky., 1620–1631.

Rittmann, B. E., and McCarty, P. L. (2001). *Environmental biotechnology: Principles and applications*, McGraw-Hill, New York.

Ruhs, A. (2006). "Zinc and copper toxicity thresholds on *Cellulomonas flavigena*." MS thesis, Colorado School of Mines, Golden, Colo.

Schafer, D., Schafer, W., and Kinzelbach, W. (1998). "Simulation of reactive processes related to biodegradation in aquifers: 2-model application to a column study on organic carbon degradation." *J. Contam. Hydrol.*, 31(1–2), 187–209.

Speece, R. E. (1996). *Anaerobic biotechnology for industrial wastewaters*, Archae, Nashville, Tenn.

Sylvia, D., Fuhmann, J., Hartel, P., and Zuberer, D. (1998). *Principles and applications of soil microbiology*, Prentice-Hall, Upper Saddle River, N.J.

TAPPI. (1999). "TAPPI test method T207 OM-99: Water solubility of wood and pulp." *TAPPI test methods*, Technical Association of the Pulp and Paper Industry, Atlanta.

Templeton, D., and Ehrman, T. (1995). *Determination of acid-insoluble lignin in biomass: Chemical analysis and testing task laboratory analytical procedure (LAP-003)*, National Renewable Energy Laboratory, Golden, Colo.

Tuttle, J. H., Dugan, P. R., and Randles, C. I. (1969). "Microbial sulfate reduction and its potential utility as an acid mine water pollution abatement procedure." *Appl. Microbiol.*, 17(2), 297–302.

Utgikar, V., Tabak, H., Haines, J., and Govind, R. (2003). "Quantification of toxic and inhibitory impact of copper and zinc on mixed cultures of sulfate-reducing bacteria." *Biotechnol. Bioeng.*, 82, 306–312.

Van Soest, P. J. (1994). *The nutritional ecology of the ruminant*, 2nd Ed., Cornell University Press, Ithaca, N.Y.

Vasiliev, V. B., Vavilin, V. A., Rytov, S. V., and Ponomarev, A. V. (1993). "Simulation model of anaerobic digestion of organic matter by a microorganism consortium: Basic equations." *Water Resour.*, 20(6), 714–725.

Vavilin, V. A., Lokshima, L., Jokela, J., and Rintala, J. (2004). "Modeling solid waste decomposition." *Bioresour. Technol.*, 94(1), 69–81.

Venot, C. (2008). "Evaluation of passive treatment of mining influenced water by biochemical reactors using substrate characterization and stoichiometric analysis of sulfate reduction." MS thesis, Colorado School of Mines, Golden, Colo.

Wakao, N., Takahashi, T., Sakurai, Y., and Shiota, H. (1979). "A treatment of acid mine water using sulfate-reducing bacteria." *J. Ferment. Technol.*, 57(5), 445–452.

Waybrant, K. R., Blowes, D. W., and Ptacek, C. J. (1998). "Selection of reactive mixtures for use in permeable reactive walls for treatment of mine drainage." *Environ. Sci. Technol.*, 32(13), 1972–1979.

Western Governors Association (WGA). (1998). "Cleaning up abandon mines: A Western partnership." ⟨http://www.westgov.org/wga/publicat⟩ (June 1, 2010).

Westrich, J. T., and Berner, R. A. (1984). "The role of sedimentary organic matter in bacterial sulfate reduction: The G model tested." *Limnol. Oceanogr.*, 29(2), 236–249.

Whitehead, P. G., Cosby, B. J., and Prior, H. (2005). "The Wheal Jane wetlands model for bioremediation of acid mine drainage." *Sci. Total Environ.*, 338(1–2), 125–135.

Widdel, F. (1988). "Microbiology and ecology of sulfate and sulfur-reducing bacteria." *Biology of anaerobic microorganisms*, A. J. B. Zehnder, ed., Wiley-Liss, New York, 469–486.

Wildeman, T. R., Gusek, J. J., Miller, A., and Fricke, J. (1997). "Metals, sulfur, and carbon balance in a pilot reactor treating lead in water." *In situ and on-site bioremediation*, Battelle, Columbus, Ohio, 473–495.

Zehnder, A. J. B., and Stumm, W. (1988). "Geochemistry and biogeochemistry of anaerobic habitats." *Biology of anaerobic microorganisms*, A. J. B. Zehnder, ed., Wiley-Liss, New York, 1–38.